RADC-TR-83-269
In-House Report
December 1983

A STATISTICAL CHANNEL MODEL FOR ADAPTIVE HF COMMUNICATIONS VIA A SEVERELY DISTURBED IONOSPHERE

D. Mark Haines

APPROVED FOR PUBLIC RELEASE; DISTRIBUTION UNLIMITED

DTIC
ELECTE
MAY 1 8 1984
S   D
B

ROME AIR DEVELOPMENT CENTER
Air Force Systems Command
Griffiss Air Force Base, NY 13441

84   05 21   004

SECURITY CLASSIFICATION OF THIS PAGE *(When Data Entered)*

REPORT DOCUMENTATION PAGE	READ INSTRUCTIONS BEFORE COMPLETING FORM

1. REPORT NUMBER	2. GOVT ACCESSION NO	3. RECIPIENT'S CATALOG NUMBER
RADC-TR-83-269	*AD-A142 237*	

4. TITLE *(and Subtitle)*	5. TYPE OF REPORT & PERIOD COVERED
A STATISTICAL CHANNEL MODEL FOR ADAPTIVE HF COMMUNICATIONS VIA A SEVERELY DISTURBED IONOSPHERE	In-House Report
	6. PERFORMING ORG. REPORT NUMBER

7. AUTHOR(s)	8. CONTRACT OR GRANT NUMBER(s)
D. Mark Haines	

9. PERFORMING ORGANIZATION NAME AND ADDRESS	10. PROGRAM ELEMENT, PROJECT, TASK AREA & WORK UNIT NUMBERS
Rome Air Development Center (EEPI) Hanscom AFB, Massachusetts 01731	62702F 46001609

11. CONTROLLING OFFICE NAME AND ADDRESS	12. REPORT DATE
Rome Air Development Center (EEPI) Hanscom AFB, Massachusetts 01731	December 1983
	13. NUMBER OF PAGES
	28

14. MONITORING AGENCY NAME & ADDRESS *(if different from Controlling Office)*	15. SECURITY CLASS. *(of this report)*
Rome Air Development Center (EEPI) Hanscom AFB Massachusetts 01731	Unclassified
	15a. DECLASSIFICATION/DOWNGRADING SCHEDULE

16. DISTRIBUTION STATEMENT *(of this Report)*

APPROVED

~~Recommended~~ for public release, distribution unlimited.

17. DISTRIBUTION STATEMENT *(of the abstract entered in Block 20, if different from Report)*

18. SUPPLEMENTARY NOTES

RADC Project Engineer: D. Mark Haines, RADC/EEPI

19. KEY WORDS *(Continue on reverse side if necessary and identify by block number)*

Adaptive HF	DPSK
Ionospheric propagation	Spread spectrum
Channel coherence	Pulse compression
High frequency	Channel dispersion
Channel model	

20. ABSTRACT *(Continue on reverse side if necessary and identify by block number)*

Motivation for the resurgence of interest in improving HF communication is presented. This includes the continued widespread use of the HF band, and the new technology that now makes it feasible to vastly improve the historically poor quality of communications in this band. Non-conventional HF techniques or systems are classified into four general categories according to the technical specialties that spawned them. These categories are Adaptive Frequency Management, Digital Waveform Processing, Networking, and Adaptive Antennas.

DD $^{\text{FORM}}_{\text{1 JAN 73}}$ 1473

20. Abstract (Contd)

A 15 parameter channel model is presented which forms the basis for the on-going RADC measurement program. These parameters address the dispersion and dynamics of time, frequency and spatial distortion imposed by the skywave channel.

Next, measurement techniques are evaluated for characterization of these parameters, resulting in the selection of a six station Arctic network of wideband pulse compression (matched filter) channel probes. A description of waveform generation, receiver signal processing and the program plans and schedule are presented.

Contents

3

Illustrations

A Statistical Channel Model
for Adaptive HF Communications
via a Severely Disturbed Ionosphere

1. INTRODUCTION

Although HF skywave channels have been used routinely for several decades and the shortcomings of this conventional communications mode have been well documented, there is now a growing interest in developing "smart radios" capable of overcoming most of the shortcomings that now exist. Due to the rapid development of low-cost miniaturized computers, the development of radios (with embedded computers), which drastically reduce channel outage rates, signal distortion, and interference, is continually becoming more feasible and attractive. There are a wide variety of techniques that could be employed by these "smart radios" and these are collectively referred to as Adaptive HF technology. This paper will categorize these techniques and outline a research program based on experimental measurements, which will assess the impact of the dynamic propagation characteristics of the ionosphere on each class of techniques.

The technology to adaptively select operating frequencies that provide optimum received signal-to-noise ratios (SNR) has been demonstrated and continues to become more feasible for general use. The U.S. military is currently employing a technique based on FM/CW chirpsounders and scanning receivers (interference monitors) in the AN/TRQ-35 frequency management system. In a totally separate effort Collins Radio (Rockwell International) has developed a system that

probes allocated frequencies using an addressable FSK code to initiate contact and monitor network connectivity. Other notable technologies that have been demonstrated are adaptive equalization modems, which remove signal distortion and intersymbol interference, and adaptive antenna arrays, which reduce interference by optimal control of the radiation patterns. As a first cut at categorizing the techniques involved, the following defines those adaptive functions that hold the most promise for significantly increasing the quality and reliability of HF communications systems:

a. Adaptive Frequency Management - Finding and using the frequency that provides the best SNR by making real-time probe measurements of propagation conditions and automatically assessing noise and interference levels.

b. Digital Waveform Processing - This broad area includes adaptive narrowband interference (NBI) cancelling, spread spectrum coding and detection (including frequency hopping), anti-distortion processing using adaptive equalizers, bit interleaving, and error detection and correction coding of information bits.

c. Networking - The ability to automatically identify and gain access to, via a relay or relays, alternate geographic signal routes to bypass ionospherically induced propagation outage conditions on the great circle skywave path. This is also called path diversity.

d. Adaptive Antennas - Phased array antennas capable of varying the phase and amplitude characteristics of their elements to achieve attenuation of unwanted signal sources and enhancement of the desired signal.

The feasibility of implementing these adaptive techniques depends heavily on the variations of spatial, frequency, and time correlation of the received signal, having been distorted in these dimensions by the propagation medium. However, the statistical distributions of several of these critical parameters are insufficiently described in any literature from past research. The current program at RADC (entitled Adaptive HF Propagation Studies) is aimed at completing the knowledge of these propagation dynamics and providing statistical data (in handbook form) that will allow methodical optimization of adaptive systems.

Specifically, the RADC Adaptive HF experimental measurement program will produce probability density functions (pdf's) for six critical HF channel parameters and nine first derivatives of these parameters dealing with the time, frequency, and spatial response of the channel under benign (quiet) conditions, moderately disturbed conditions, and severely disturbed conditions. These six parameters are shown in Figure 1 as the Gross and Fine Parameter for each domain (time, frequency, and spatial). The first derivatives are also described. The communication links to be measured include several transauroral and transpolar paths to insure that intense and dynamic conditions will be encountered on a routine basis (see Figure 2).

	1. Time	2. Frequency	3. Spatial
a. Gross	Pdf's* of received signal strength at 0.5, 0.8, and 0.95 times MUF (in dBm)	Pdf's* of MUF (maximum) useable frequency)	Pdf's* of correlation coefficient for signal level received via 30°, 60°, and 90° azimuth separation.
b. d(Gross)/dt	Rate of degradation/recovery of signal level at optimum frequency (that is, dB/min)	Pdf's* of rate of change of MUF value (that is, MHz/min)	Change of level of correlation. Pdf's* will have parameters in percent/min.
c. Fine	"Black box" system impulse response of HF channel. Pdf's* will show the duration of impulse response in msec at 0.5, 0.8, and 0.95 times the MUF. The lease coherent 10 percent of signal power will be ignored.	Wideband channel transfer function at fixed center frequency. Pdf's* will show in-band peak-to-null ratio, and 3-dB null bandwidth.	Angle-of-arrival spread due to skywave side scatter from ionospheric irregularities. Pdf's* will show angle spread of 90 percent of signal power.
d. d(Fine)/dt	Drift in propagation delay (group path delay). Will be measured as Doppler components using data from block 2.e. scaled to show μs/sec.	3-D plots will display the change in the transfer function as a function of time.	Pdf's* will show angle of arrival variation rate (deg/sec) of the apparent phase center.
e. d(Fine)/df	Pdf's* will show difference in propagation delays at various frequency separations (for example, 100, 200, 500 KHz, and 1 MHz) around FOT.	Pdf's* will show the maximum Doppler spread in Hz included in the most coherent 90 percent of received power.	Pdf's* will show correlation coefficient of concurrent source field intensities (over elevation and azimuth) for various separations in frequency (from 0-10 KHz separations).

*See page 9.

Figure 1.   Measurement Objectives.   (See Section 2 for complete descriptions)

7

CHANNEL PROBE/SOUNDING NETWORK
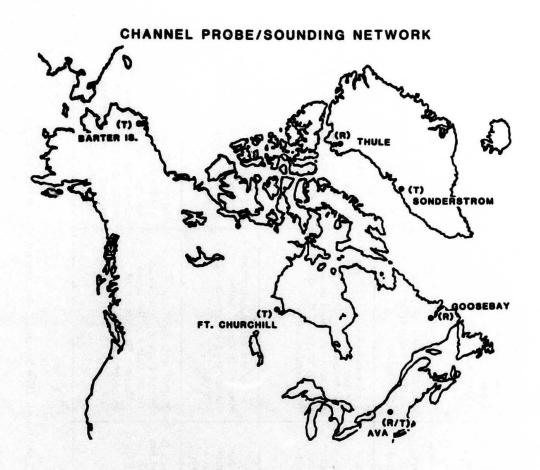
Figure 2. Wideband Adaptive Arctic HF Testbed

The channel model being statistically characterized by these measurements is a linear system or "black box" model that produces an output function (Y) for any input function (X). For these measurements X can always be expressed as an impulse function in the time, frequency, or position (spatial) domains. Such a set of pdf's should enable specific trade-offs to be made for network architecture, transmitter power, equalizer specifications, type and complexity of signal processing, waveform design, specific implementation of adaptive antennas, channel probe techniques, channel acquisition protocols, etc.

The six characteristic parameters and their first derivatives can be organized in a matrix as in Figure 1 and will be described in detail in the next section. These 1-D parameters were chosen to minimize the ambiguity inherent in multi-dimensional functions and also to make the data applicable to the widest range of

systems and applications by allowing modeling of different combinations of system parameters.

2. MEASUREMENT OBJECTIVES

2.1 Time Domain Channel Characterization
(Subparagraph numbers correspond to parameter locations on Figure 1)

2.1.a Gross time dependence - Pdf's* of signal levels in dBm will be prepared from data at 0.5, 0.8, and 0.95 times the current value of the MUF (maximum usable frequency) on each link. This data will be of some interest by itself in selecting transmitter power and processing gain for reliable links, but it will also be the basis for the spatial measurement of 2.3.a.

2.1.b Rate of channel deterioration/recovery - For a completely frequency adaptive system that can track variations in the MUF (rates of variation are addressed in 2.2.b) the parameter of interest is the rate of change of path loss on the frequency of optimum transmission (FOT, for example, 0.8 or 0.95 times the MUF). Therefore, these pdf's* will be displayed as dBm/min for each link measured, while being automatically adjusted (floating) in frequency for variations in MUF.

2.1.c Fine time dependence - This will be a compilation of parameters relating to the linear system impulse response of the HF channel being measured. Data will be displayed in 3-D composites, such as Figures 3a and 3b, that are, respectively, variation with time, and variation with frequency (the latter is also known as an ionogram). Also, pdf's* will be prepared showing the distribution of response duration (typically 0 to 5 msec); that is, the maximum time-delay spread spanned by the most coherent 90 percent of the received signal power. It should be noted here that the two probe techniques to be implemented during this measurement program are the mathematical equivalent of transmitting a 10-μsec RF pulse envelope and measuring the pulse spreading at the receiver.

They are both, therefore, a direct measurement of the impulse response (also Green's function or spreading function) characterizing the system properties of the skywave channel. Since there is so much information derived from these measurements, several other parameters (for example, coherence of individual skywave modes, amplitude relationship of identifiable modes such as 1F and 2F, fading rate of individual modes, etc.) will be examined. These impulse response

---

*Pdf's will be prepared from pre-sorted data records such that separate pdf's will be available to characterize sunrise, midday, sunset, and midnight conditions for each season, at 0.5, 0.8, and 0.95 times the current MUF and also exclusively for benign, moderately disturbed, and severely disturbed ionospheric conditions.
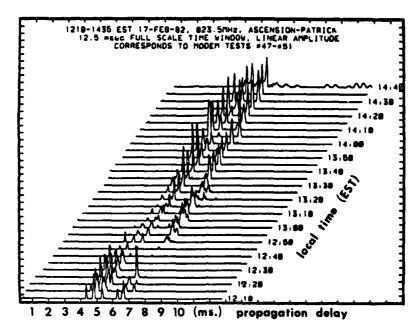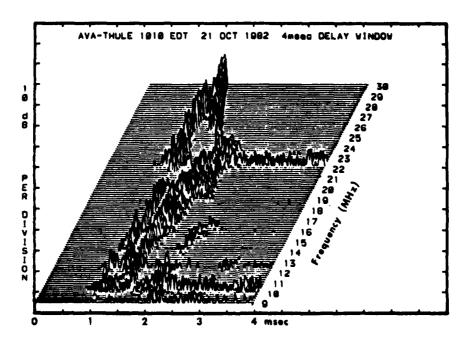
Figure 3a. Impulse Reponse vs Time

Figure 3b. Impulse Reponse vs Frequency

10

measurements will establish the feasibility of building adaptive data rate modems; they will also characterize attainable spread spectrum processing gains, and required channel equalization filter length (maximum delay).

2.1.d Rate of change of impulse response - This parameter will be obtained from the Doppler spread measurements available during Phase II of our measurement program using a Wideband Channel Probe. By scaling the observed Doppler shifts based on the transmitted center frequency the rate of change of the group path delays can be computed. Pdf's* will be prepared showing delay length changes in units of μsec/sec. This data will comprise a benchmark for evaluation of adaptive equalizer tracking (convergence) rates and comparison of noncoherent modulation systems (for example, FSK, DPSK) vs coherent modulation (for example, coherent PSK).

2.1.e Time delay vs frequency - The virtual reflection height[1] of HF skywave signals varies with frequency. Therefore, broadband signals experience a continuous time dispersion and frequency-hopped signals a discontinuous shift possibly causing a loss of synchronization. Pdf's* will be prepared showing delay spreads (of a single propagating mode) over 100, 200, 500, and 1000 kHz.

2.2 Frequency Domain Channel Characterization

2.2.a Gross frequency dependence - Pdf's* will be prepared showing the observed values of MUF on each link. This data will determine optimum distributions of channel access (that is, network control) frequencies for various network protocols and geographic locations. It will also affect selection of the VHF extension option (ability to operate above 30 MHz) for various users by indicating how often and under what conditions these frequencies would be useful.

2.2.b Rate of change of MUF with time - Pdf's* will be prepared showing the distribution of changes in the MUF (that is, MHz/min). This will indicate required propagation update (that is, retransmission of probing or sounding signals) rates for real-time adaptive frequency selection systems.

2.2.c Frequency response - Since the various multipath components of an HF channel arrive with random phase relationships (uniform distribution of phase angle) the impulse response is complex (that is, must be represented as I and Q components). The channel's frequency response will be measured directly during Phase II by spectrum analyzing the received spread spectrum (20 or 200-kHz bandwidth pseudo noise signal). The width and depth of nulls in the frequency response will set performance limits on narrowband FSK performance and also help select parameter ranges for adaptive equalizers.

1. Davies, K. (1965) Ionospheric radio propagation, National Bureau of Standards Monograph 80, U.S. Dept. of Commerce.

2.2.d Frequency response vs time - 3-D plots will display variations of 2.2.c over periods of a few seconds with a 50-msec update rate.

2.2.e Variations in frequency response - The frequency spread of Doppler components measured from a CW transmission will define the rate of change of the complex frequency response of the channel. Since two multipath components will change from in-phase summation to out-of-phase cancellation for each π radian change in relative phase, the frequency difference between these components specifies this fading rate directly (frequency is expressed in radians/sec). Therefore, the maximum fading rate on a channel is the inverse of the maximum Doppler spread. To maintain practical significance this data will represent only the most coherent 90 percent of signal power. Pdf's* of this parameter will directly specify required channel equalizer convergence rates.

2.3 Spatial Domain Channel Characterization

2.3.a Azimuthal correlation of path loss - A critical parameter in evaluating the effectiveness of a relaying strategy for circumventing channel outages is the degree of independence of the various available signal routes. Variations in MUF and path loss due to range are quite predictable from geometry considerations, but have a less predictable variation superposed over the deterministic variation due to the physical displacement of the ray path. This same displacement variability (that is, the signal passes through a different section of the ionosphere) can be observed by approaching the receiver from a different azimuth at approximately the same range. This measures the decorrelation of ionospheric properties as a function of distance between "reflection points" without the complication of the range variation.

Pdf's* will be prepared showing the cross correlation of signal levels for each of 30°, 60°, and 90° azimuth separations. The frequencies at which the signal levels are measured will again be 0.5, 0.8, and 0.95 times the MUF (the same raw data as parameter 1.a). This normalization relative to the path MUF will eliminate the effect of expected variations in MUF resulting from path midpoints being in different sunlight illumination regions. This data base will enable network designers to realistically predict overall connectivity for various levels and complexity of network architectures.

2.3.b Rate of change of path-to-path correlation - Short-term (minutes) and long-term (hours) variations in path correlation will be investigated to determine an optimum "try again" interval for occasions when no connectivity to the intended receiver can be found.

---

*See note on page 9.

2.3.c Angle-of-arrival spread - Since the ionosphere is not a smooth spherical surface, but often has extreme irregularities, a skywave signal will contain scattered components that traveled via a path different from the great circle. Ray trace simulations performed on computer-generated model ionospheres have shown arrival angle dispersion of over 10°.[2,3] Such variations make conventional null steering ineffective. Pdf's* of angular spread of the 90 percent power scatter region will be made as well as actual intensity maps of cases of particular interest. These data will establish the feasibility of nulling the entire region of the apparent interference source.

2.3.d Change in apparent angle-of-arrival vs time - For coherent scattering from a region smaller than the resolution of the phased array receiving antenna there is only one apparent source that could produce the phase front observed at the antenna. However, this source will move rapidly as the many "wavelets" from the scattering region sum to a different phase front. If this phase center can be adaptively tracked a deep null can be held on the scattering source. The feasibility of building such a system will depend on the rate of movement of that phase center. This can be measured by direction finding on the source several times per second, using the complex amplitudes at each antenna element in a phased array to refine the apparent direction to greater accuracy than a resolution cell.

2.3.e Change in apparent angle-of-arrival vs frequency - Images of the scattering region power distribution will be computed simultaneously on two "zero bandwidth" tones separated by a variable frequency difference. Cross power correlation of these images vs frequency separation will be investigated. This data will establish the feasibility of nulling broadband signals (for example, noise jammers).

2.4 Interference and Noise

All the measurement objectives described above produce an absolute measurement rather than a SNR or bit error rate probability. It was decided that measurements that ignore noise were more universally applicable since unwanted signals depend greatly on receiver location, locally generated noise, and on the level of enemy efforts to disrupt communications links. On top of these manmade conditions, the amount of noise that propagates to a receiver depends on the path loss

---

*See note on page 9.

2. Sales, G.S., Videburg, J., and Varad, R. (1975) DASSM Project-High Latitude Aircraft HF Propagation Experiment, AFCRL-TR-75-0290, AD A015764.

3. Washburn, T.W., and Sweeney, L.E., Jr. (1976) Ionospheric Wavefront Coherence Influence on Array Sidelobe, Stanford Research Institute Tech Report #34, SRI Project 4062.

13

and MUF in the same manner as the desired signal does. A statistical estimate for this propagated component of noise and/or jamming can be derived from our propagation data, while local noise must be measured at actual receiver sites. In conclusion, noise levels are critically important, but must be treated on the basis of the specific system used and its operating location and mission. The propagation data compiled during this measurement program will give a good estimate of signal levels, which when complemented by local noise measurements and an ECM threat model, will enable realistic design of link margins and connectivity rates.

3. MEASUREMENT APPROACH

Equipment fielded to make these measurements must be highly reliable, easily operated, and require minimal attendance, since project personnel will not be manning the sites. Also, since these sites will be used for on-air testing of Air Force prototype and production systems the measurement equipment must serve the dual purposes of gathering the research data outlined in Section 2 and performing real time test-support by characterizing the HF channels during system testing.

3.1 Time Domain and Frequency Domain Measurements

Since a linear system model of the HF channel is being employed, the desired output of the channel probe system is an impulse response and frequency response at a fixed center frequency. This fixed center frequency must also be automatically retuneable (from 2 to 60 MHz) to scan the entire potentially useful HF spectrum. Therefore, two operating modes will be employed using the same system and waveform, a sounder mode and a channel probe mode. The sounder mode however, is just an automatically controlled sequence of channel probe measurements covering a predetermined range of center frequencies.

Conventional HF channel measurement systems are the pulse sounder and FM/CW chirpsounder. As their names imply they run in a sounder mode but not a channel probe mode. In the sounder mode they only revisit a particular center frequency once per several minutes; much too slow to track many of the propagation parameters of interest. Also, existing sounder systems only operate up to 30 MHz. Both techniques, however, can be modified to operate as channel probes.

3.1.a Pulsed channel probe - This would require the pulse sounder to stay on a fixed frequency and transmit 10- to 100-μsec RF pulses at less than 100-Hz pulse repetition frequency (PRF). The pulse length determines the time resolution

14

of the measurement (100 μsec is sufficient to evaluate a conventional SSB channel), while the low PRF is required to eliminate pulse-to-pulse ambiguity from multi-path returns. A 100-Hz PRF provides 10 msec of unambiguous impulse response. A complex amplitude response can be measured by processing an I and Q channel. Due to channel induced Doppler, coherent averaging in excess of 100 msec is not feasible. Intra-pulse phase coding allows more processing gain, but this technique is the basis for the Direct Sequence (DS) and matched filter systems covered in paragraphs 3.1.c and 3.1.d.

3.1.b FM/CW channel probe - The "chirp channel probe" typically sends a train of pulses (up to 100 percent duty cycle), each of which is swept in frequency through the fixed frequency of interest. The total chirp bandwidth is 20 to 100 kHz, while the PRF is again less than 100 Hz. Since the chirp waveform is a type of intrapulse coding the receiver provides processing gain, which reduces the requirement for transmitter power (for example, 100 Watts is sufficient for most forward scatter applications). Demodulation at the receiver is performed by a chirping local oscillator (LO), which sweeps in frequency at precisely the same rate as the transmitter. Therefore, all Intermediate Frequencies (IF) are fixed frequency signals with a spread of spectral components offset in frequency in proportion to the propagation delay experienced by various ray components in the received signal. The noncoherent channel impulse response (that is, magnitude of the complex response) can be represented by the power spectrum of this IF signal. A conventional HF chirpsounder as will be used in Phase I of the RADC program does exactly the same thing except that the bandwidth covered is 28 MHz rather than 20 to 100 KHz, and the PRF is 1/5 min.

3.1.c DS channel probe - The next alternative to be considered is a synchronous DS spread spectrum probe. All DS systems require a known spreading code p(t), preferably with very low autocorrelation sidelobes, that is, ideally this code would have the following property:

$$\overline{p(t)\,p(t-d)}^T = \int_0^T p(t)\,p(t-d)\,dt = \begin{array}{l} 0 \text{ for } d \neq 0 \\ 1 \text{ for } d = 0 \end{array} \quad , \tag{1}$$

where the integration period, T, indicates an average over an interval T = one code length. For very long codes small partial correlation responses (that is, time sidelobes) become insignificant since they will probably fall below the receiver noise floor, making a pseudo-random DS code (which is not optimized for time sidelobes) acceptable. The pseudo-random codes are preferable for secure communication systems since there are nearly an infinite number of

15

practical code combinations, but for a propagation probe system we can select a unique code with optimal correlation properties. One such code is a periodic maximal length sequence[4] of $2^n - 1$ bits per code repetition. This sequence is trivial to generate using a TTL shift register and one exclusive OR gate as shown in Figure 4.[5] The code rate and thus its bandwidth are variable simply by changing the clock frequency f_c.
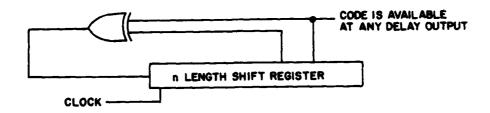

Figure 4. Maximal Length Code Generator

The length of the code depends upon which shift delays[5] are chosen to feedback to the input giving a code length $N = 2^n - 1$, where n is the most delayed shift involved in the feedback path. (Note that $T = N/f_c$.) The auto-correlation of this sequence is

$$\overline{p(j)\,p(k)}^T = \int_0^T p(j)\,p(k) = \begin{cases} -1/N & \text{for} \quad j \neq k \\ 1 & \text{for} \quad j = k \end{cases} \quad . \tag{2}$$

For instance, if n = 10 (N = 1023) the time sidelobes of this code are over 60 dB below the peak. This code can be transmitted by bi-phase modulating a carrier, (PSK or phase reversal modulation) producing s(t), at the center frequency to be probed resulting in the transmitted spectrum of Figure 5. The transmitter system can be quite simple as illustrated in Figure 6a (our actual transmitter system is shown in Figure 7, the receiver system in Figure 8). The received signal is a delayed replica of the transmitted signal except, in the case of multipath channels, for the addition of superposed replicas having propagation delays (τ_i) and various

---

4. Brookner, E. (1977) Radar Technology, Artech House, Inc., Chapter 8.

5. Butler, F. (1975) Pseudo random binary sequence generators, Wireless World, February.

amplitudes (a_i). Therefore, using a linear system channel model the general expression for the received signal is:

$$r(t) = \int h_{channel}(u) \, s(u - t) \, du$$

$$= \int \sum_i a_i \, \delta(u - \tau_i) \, s(u - t) \, du$$

$$= \sum_i a_i \, p(t - \tau_i) \sin [\omega_c t + \phi_i(t)] \quad .$$
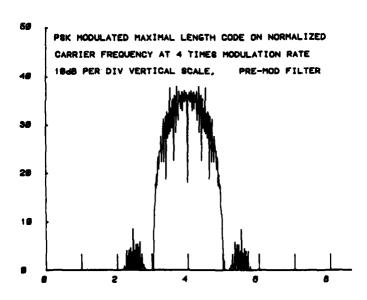
Figure 5. Spread-Spectrum Waveform Spectrum

$s(t) = f_c(t)p(t)$

Ideally:

$$\overline{p(t-a)p(t-b)} = \begin{cases} 0 & \text{for } a \neq b \\ 1 & \text{for } a = b \end{cases}$$

For Maximal Length Sequence:

$$\overline{p(t-a)p(t-b)} = \begin{cases} -1/N & \text{for } a \neq b \pm nT \\ 1 & \text{for } a = b \pm nT \end{cases}$$

If $N = 1023$ then Peak/Sidelobe = 60 dB
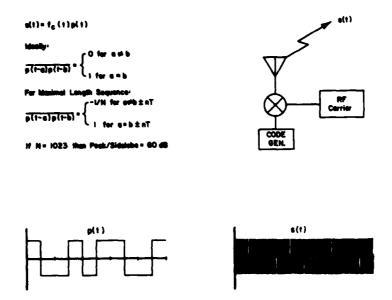
Figure 6a. Spread Spectrum Waveform

$A_0 = \sum_i a_i f_c(t-d_i)p(t-d_i)$

$A_1 = \sum_i a_i p(t-d_i)$

$A_2 = \sum_i \overline{a_i p(t-d_i)p(t-\Delta)}$

$$A_2 = \begin{cases} a_i & \text{for } \Delta = d_i \pm nT \\ -a_i/N & \text{for } \Delta \neq d_i \pm nT \end{cases}$$

$B_0 = \sum_i a_i f_c(t-d_i)p(t-d_i)$

$B_1 = \sum_i a_i p(t-d_i)$

$B_2 = \int_0^T \sum_i a_i p(u-d_i)p(u-t)du$

$$B_2 = \begin{cases} a_i & \text{for } t = d_i \pm nT \\ -a_i/N & \text{for } t \neq d_i \pm nT \end{cases}$$
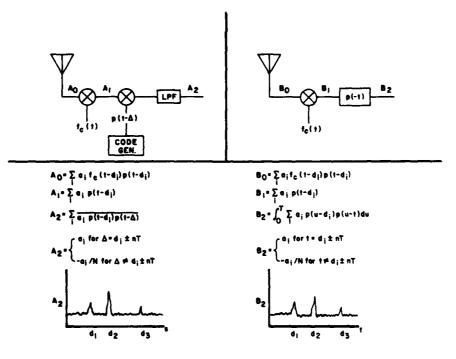
Figure 6b. Receiver Processing Options

18
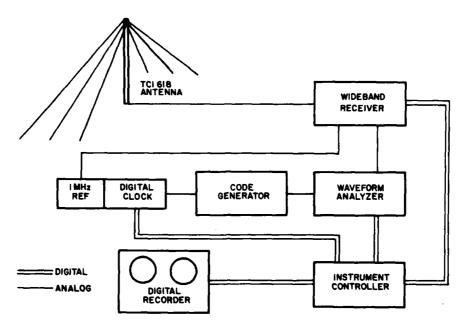
Figure 7 Channel Probe Receiver Site
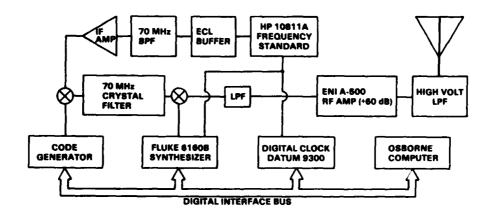
Figure 8. Wideband Channel Probe Transmitter

This expression reflects the fact that on a multipath channel the carrier is a summation of sinusoids of random phase, the received envelope may be a summation of delayed code modulation envelopes, and each multipath component may have an arbitrary amplitude. Since the multipath phases are random a quadrature demodulation technique is required and, saying this much, we will eliminate the

19

carrier term from future expressions. Due to the correlation properties of the code, the output of the demodulator and low-pass filter in Figure 6a is vanishingly small unless a controllable synchronization delay (Δ) is set to match one of the propagation delays on the channel, that is,

$$A_2 = a_i \overline{p(t - \tau_i)\, p\,(t - \Delta)} = \begin{cases} a_i & \text{for} \quad \tau_i = \Delta \\[2mm] 0 & \text{for} \quad \tau_i \neq \Delta \end{cases} \tag{3}$$

Therefore, by successive measurements at all delay settings of interest $h_{channel}(t) = A_2(\Delta)$ the impulse response of the channel can be measured as the demodulated output, $h(\tau_i)$ (a DC voltage level) for each time delay Δ_i. The major disadvantage of this technique is that there is no assurance that the channel response measured at time Δ_i will still be valid when Δ_j is being measured. Since the rate of change of the impulse response parameters is one of the measurements required of the system, such an uncertainty cannot be tolerated. The following technique has been selected to remedy this and, as shown later, makes all delay measurements simultaneously, but is the mathematical equivalent to synchronous DS detection.

3.2 Matched Filtered Detected Spread Spectrum Probe

The transmitted signal will be identical to that of the previous technique except that the code will be modulated onto the carrier differentially (DPSK) rather than directly, allowing the received signal to be nonsynchronously phase detected.[6] Nonsynchronous detection eliminates the effect of Doppler shifting on the phase of the baseband output. Therefore, the baseband can be coherently averaged for on the order of 1 min, where synchronous detection would be limited to about 100-msec averaging duration. The DPSK demodulator will produce (for a multipath channel) a baseband output,

$$b(t) = \sum_i a_i\, p(t - \tau_i) \tag{4}$$

where a_i is the amplitude of the channel response at time delay τ_i. This output will then be sampled into a digital waveform analyzer where it will be coherently averaged as many times as required to provide the desired SNR. In order to

6. Peebles, P. Z., Jr. (1976) Communication System Principles, Addison Wesley, Sections 4.10 and 8.8.

20

determine the channel impulse response, the waveform analyzer can be directed via its interface bus to perform a convolution of this sampled data with a digital matched filter. Note that the convolution can be performed by complex multiplication of the Fourier transformed array by the transform of the code or it can be performed by direct digital convolution.[7] The matched filter has an impulse response that is the maximal length sequence code reversed in time.[8] That is,

$$h_m(t) = (p(-t) \quad . \tag{5}$$

The waveform analyzer will perform a digital convolution of this matched filter with the sampled receiver baseband resulting in a matched filter output,

$$y_m(t) = \int_0^T b(t) h_m(t - u) \, du = \int_0^T \sum_i a_i p(u - \tau_i) h_m(t - u) \, du \quad . \tag{6}$$

Using Eqs. (5) and (2) we see that y(t) is itself a correct representation of the non-coherent impulse response of the skywave channel (1.c in Figure 1),

$$y(t) = h_{channel}(t) = \sum_i a_i \int_0^T p(u - \tau_i) \, p(u - t) \, du$$

$$= \sum_i a_i \, \delta(t - \tau_i) \quad .$$

Therefore, simply by waiting until $t = \tau_i$ the output of the matched filter will automatically (that is, no synchronization or signal present indication is required) be a_i. The moment that the end of the last code bit is transmitted is defined as $t = 0$. Since a periodic code is being used it is important that there is only one $t = 0$ during the entire duration of the channel response such that all a_i's and τ_i's can be referenced unambiguously to the proper $t = o$. Therefore both of our operating modes have code lengths in excess of 10 msec.

---

7. Oppenheim, A.V., and Schaffer, R.W. (1975) Digital Signal Processing, Prentice Hall, Chapter 3.2.

8. Thomas, John B. (1969) An Introduction to Statistical Communication Theory, Wiley, Chapt. 5.1.

21

A computer simulation of a coherently demodulated PSK multipath RF signal, which is matched filter processed by a 127 length $(N = 2^7 - 1)$ maximal length code, is shown as Figure 9. The RF signal was time dispersed by discrete multipath delays and a 0-dB SNR was created by adding a random number to each sampled value. This simulation demonstrates the tremendous processing gain offered by the matched filter, and also demonstrates the effect of random phase components on a synchronously detected signal.

INPUT SNR = 0 dB   1st MODE vs LO PHASE = 0°
CODE LENGTH = 127   2nd MODE vs LO PHASE = 90°

0 ——————————————————————— 12.7 msec

MAGNITUDE OF IMPULSE RESPONSE $(I^2 + Q^2)^{1/2}$

0 ——————————————————————— 12.7 msec

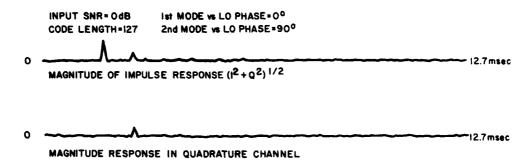MAGNITUDE RESPONSE IN QUADRATURE CHANNEL

Figure 9. Spread Spectrum Processing Gain

The Fourier transform of the sampled IF signal is also of interest in the planned measurement program since it directly measures the channel transfer function (2.c in Figure 1). Sequential measurements of the IF spectrum (for example, each 50 msec) will characterize the rate of change of the channel transfer function (2.d in Figure 1), since the spectrum of a system output with white noise input is the transfer function.[6] The dynamic nature of these selective fades in the transfer function is shown in Figure 10 in a 4-sec sequence of a phase-modulated SSB data modem baseband (same signal as Figure 5).

The availability of both time domain and frequency domain data from the same transmitted waveform and the simultaneous processing of all time delays in the impulse response are the major advantages of matched filter processing over the other techniques. The fine spatial measurements required for objectives 3.c, 3.d, and 3.e will be accomplished at a later time under Phase 3 of the RADC Adaptive HF program. Therefore, a specific description of measurement techniques will be described in later reports. The spatial parameters were included in Figure 1 for completeness, but since the hardware is still in trade-off analysis it would be premature to try to report on findings.
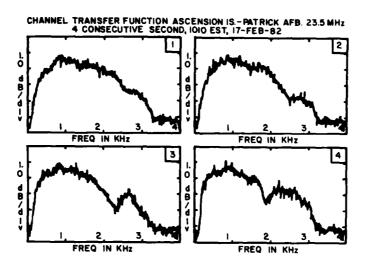
22

CHANNEL TRANSFER FUNCTION ASCENSION IS.-PATRICK AFB. 23.5 MHz
4 CONSECUTIVE SECOND, IOIO EST, 17-FEB-82

Figure 10. Variability of Channel Response

4. PROGRAM PLANS

The program objectives outlined in Figure 1 are all to be accomplished during three program phases. The approximate operational periods for these phases are Phase I, 1983-1985; Phase II, 1984-1987; Phase III, 1984-1987 with Phases II and III possibly continued or reactivated in 1989-91 to characterize a more active sunspot period.

4.1 Phase I — Azimuth Diversity Experiment

Since RADC's propagation branch owned or had access to three chirpsounder transmitters and one receiver, Phase I was initiated during 1982 to collect what data could be measured with these systems. The measurement objectives fully or partially met by the chirpsounder network are, from Figure 1: 1.a (only below 30 MHz), 1.b and 1.c (below 30 MHz), 1.d (no short-term tracking, only capable of 15-min updates), 1.e, 2.a, and 2.b (15-min updates), 3.a (no data on true one-hop channels), and 3.b (15-min updates).

Sounder transmitters have been installed at Ava, N.Y., Grand Forks, N.Dak., and Barter Island, Ark. The transmitters operate sequentially for 5 min each in a 15-min cycle. All signals are received and recorded at Thule AB, Greenland. The sounders transmit a 2- to 30-MHz signal swept in frequency at 100 kHz/sec. The demodulated baseband is recorded on analog tape and spectrum analyzed

23

during processing to produce various amplitude spectral lines representing the propagation delayed components of the received signal [$\Sigma\ a_i\ \partial(t - \tau_i)$ from Section 3].

4.2 Phase II — Wideband Channel Probe Network

DPSK spread spectrum signals will be transmitted at the 500-Watt level at the sites marked T in Figure 2. Three modes will be operated:

Mode 1 - 10-kbps length 127 binary pseudo-noise code

Mode 2 - 100-kbps length 1023 binary pseudo-noise code

Mode 3 - CW tone to measure Doppler spread.

The mode, center frequency, dwell time, signal processing steps, data format, and process sequence will be controlled by a programmable instrument controller. Therefore, the operating frequencies, averaging intervals, Doppler resolution, sequencing, etc., can all be changed at will by calling the site and uploading a new program. The data collected at the receiver sites, marked R in Figure 2, will: (a) satisfy all the objectives identified in Phase I above; (b) eliminate the measurement limitations noted in parentheses in Phase I, and (c) fulfill objectives 2.c, 2.d, and 2.e.

4.3 Phase III — Spatially Adaptive Antenna Project (SAAP)

The current plan for this phase of the Adaptive HF effort is to field a single large array (approx 1 km^2) of 64 elements capable of making complex amplitude measurements on each element at four center frequencies. Signal sources will be four transmitters all within one-hop skywave range of the array, which will be capable of transmitting two "zero bandwidth" tones separated in frequency by a variable amount. From the complex amplitude measurements on the array the source field (that is, secondary scattering sources at the ionospheric "reflection" point) will be computed and thereby the degree of spatial spreading can be measured. Since the array is 2-D there will be resolution in elevation as well as in azimuth. This system will enable measurements of 3.c, 3.d, and 3.e.

5. CONCLUSION

Most of the techniques included under the general heading, Adaptive HF, are readily implemented on line-of-sight or wireline channels, however the HF channel presents several new technical challenges because of the dynamic properties of the propagation medium. In order to select feasible technologies to incorporate into modern military radios, the magnitude and rate of change of these dynamic

24

properties must be thoroughly characterized. Since there have been no high-resolution short-interval measurements of complex impulse response made under disturbed ionospheric conditions there is a need for experimental data addressing the time domain, frequency domain, and spatial domain response of the iono-spheric skyway channel. The experimental program outlined in this paper prom-ises to fill this gap in our knowledge in a way that can be readily applied to com-munication systems analysis and design.

References

1. Davies, K. (1965) Ionospheric radio propagation, National Bureau of Standards Monograph 80, U.S. Dept. of Commerce.

2. Sales, G.S., Videburg, J., and Varad, R. (1975) DASSM Project-High Latitude Aircraft HF Propagation Experiment, AFCRL-TR-75-0290, AD A015764.

3. Washburn, T.W., and Sweeney, L.E., Jr. (1976) Ionospheric Wavefront Coherence Influence on Array Sidelobe, Stanford Research Institute Tech Report #34, SRI Project 4062.

4. Brookner, E. (1977) Radar Technology, Artech House, Inc., Chapter 8.

5. Butler, F. (1975) Pseudo random binary sequence generators, Wireless World, February.

6. Peebles, P. Z., Jr. (1976) Communication System Principles, Addison Wesley, Sections 4.10 and 8.8.

7. Oppenheim, A.V., and Schaffer, R.W. (1975) Digital Signal Processing, Prentice Hall, Chapter 3.2.

8. Thomas, John B. (1969) An Introduction to Statistical Communication Theory, Wiley, Chapt. 5.1.

Acronyms

dBm - decibels relative to a milliwatt

DS   - direct sequence (code modulation technique)

FOT - frequency optimum transmission

IF   - intermediate frequency

LO   - local oscillator

MUF - maximum useable frequency

pdf   - probability density function

PRF - pulse repetition frequency

RF   - radio frequency

SNR - signal to noise ratio

MISSION
of
Rome Air Development Center

RADC plans and executes research, development, test and selected acquisition programs in support of Command, Control Communications and Intelligence (C^3I) activities. Technical and engineering support within areas of technical competence is provided to ESD Program Offices (POs) and other ESD elements. The principal technical mission areas are communications, electromagnetic guidance and control, surveillance of ground and aerospace objects, intelligence data collection and handling, information system technology, ionospheric propagation, solid state sciences, microwave physics and electronic reliability, maintainability and compatibility.